

Reinforcement of polylactic acid with bioceramics (alumina and YSZ composites) and their thermomechanical and physical properties for biomedical application

Neha Choudhary | Varun Sharma  | Pradeep Kumar

Department of Mechanical and Industrial Engineering, IIT Roorkee, Roorkee, India

Correspondence

Varun Sharma, Department of Mechanical and Industrial Engineering, IIT Roorkee, Roorkee, India.
 Email: varuns.fme@iitr.ac.in

Funding information

Science and Engineering Research Board; Uttarakhand State Council for Science and Technology

Abstract

Fused Deposition Modeling (FDM) is one of the most popular Additive Manufacturing (AM) techniques widely used in different fields, including the medical sector. FDM uses different thermoplastic polymers to fabricate the desired shapes. However, there is a need to enhance the mechanical properties of neat biopolymers with the help of reinforcements that can be used in medical applications. This work investigates the thermomechanical, physical, and biological properties of PLA-based composites fabricated using FDM. PLA-based bio-ceramics (Al_2O_3 and Yttria Stabilized Zirconia [YSZ]) filaments have been used to prepare tensile, compression, and flexural specimens. Scanning electron microscopy has been performed to reveal the fracture characteristics of the composite specimens. Besides this, the feasibility of the polymer composite for biomaterial applications has also been analyzed. The results show that PLA/ Al_2O_3 has 30.44, 55.2, and 83.73 MPa tensile, compressive, and flexural strength, respectively. The present study also shows that the reinforcement of PLA with bioceramics also led to a reduction in wear and Coefficient Of Friction (COF) at varying loads.

KEY WORDS

additive manufacturing, alumina, fused deposition modeling, PLA, YSZ

Abbreviations: β -TCP, β -tri calcium phosphate; Δm , weight loss; ABS, acrylonitrile butadiene styrene; AM, additive manufacturing; ATR-FTIR, attenuated total reflection-Fourier transform infrared spectroscopy; CAD, computer-aided design; CBS, clobetasol propionate; COF, coefficient of friction; DLP, digital light processing; DSC, differential scanning calorimetry; FDM, fused deposition modeling; FE-SEM, field emission scanning electron microscope; Hap, hydroxyapatite; LOM, laminated object manufacturing; MCC, microcrystalline cellulose; PA, polyamide; PC, polycarbonate; PCL, polycaprolactone; PEEK, polyether ether ketone; PLA, polylactic acid; PLLA, poly(L-lactide acid); PVA, polyvinyl alcohol; SLA, stereolithography; SLS, selective laser sintering; TGA, thermogravimetric analysis; VA, vanillic acid; YSZ, Yttria stabilized zirconia; w_i , initial weight of sample; w_d , degraded weight of sample.

1 | INTRODUCTION

Additive Manufacturing (AM) is a fast-growing technology for the production of 3D structures layer by layer using Computer-Aided Design (CAD). It has numerous advantages over traditional manufacturing as less production time, the ability to fabricate complex parts, near-net-shape finish, single-step process, low cost, etc.^[1] The process starts with modeling of a 3D model using the software. Then the .stl (Standard Triangularization Language) file is exported from CAD models and imported to slicing software available with the AM machines. The slicing software is used to generate the G-codes,

which the machine nozzle follows. AM has wide applications in the medical, military, automobile, aerospace, and food industries.^[2] In the medical field, initially, AM was primarily used to fabricate pre-surgical models and surgical planning. However, nowadays, it is also being used in the fabrication of orthopedic and dental implants, tissue engineering scaffolds, organ printing etc.^[3]

AM has variety of technologies, including Stereolithography (SLA), Fused Deposition Modeling (FDM), Laminated Object Manufacturing (LOM), Digital Light Processing (DLP) and Selective Laser Sintering (SLS), etc. Among all these technologies, FDM has various inherent qualities due to which it has been extensively used in the medical sector.^[4,5] The medical devices have to be made to match human anatomy. Moreover, FDM can be used to fabricate complex shapes with low cost, less time, and less material wastage. The technique uses a variety of biodegradable and biocompatible natural and synthetic polymers to fabricate bioimplants, bone grafts, medicines, etc.^[6] However, pure polymers do not meet the requirement for the clinical application of biomaterials. This adds value toward the effort in the development of novel materials. The main focus while developing new biomaterials is to have beneficial biological functions with a new set of mechanical, chemical, and physical properties.^[4] Among these, the mechanical property is the most important property for biomaterials. Many researchers have developed composite materials by combining more than one polymer and reinforcing bioceramics to enhance the product's mechanical and biological properties.^[7,8] Bioceramics are the biomaterials with biological functionality, means, which can be implanted into human body without causing any adverse effect. These ceramics interact differently inside living body, based on that they are classified into bioinert, biosorbable, and bioactive ceramics.^[9] Fused deposition of ceramics usually contains ~40% ceramics part.^[10] Nowadays, polymer loaded with ceramics has been used in the production of scaffolds for tissue engineering. Several bioceramics such as hydroxyapatite,^[11] calcium phosphate,^[12] etc., have been blended in polymers such as PLA, PVA, and PCL to achieve enhanced properties in the fabrication of 3D scaffolds.

Among these, PLA has been frequently used in the fabrication of medical devices. Its low cost and good biocompatibility make it the most suitable material for implant fabrication, drug delivery, and tissue engineering. Many researchers have reported the fabrication of scaffolds with PLA. In this regard, Mondal et al.^[13] studied the influence of Hap incorporation on PLA scaffolds. It was found that the coating of Hap on PLA increased the cell attachment and mechanical strength up to 47.16% for the fabricated scaffold. Dubinenko et al.^[14]

studied the variation of Hap weight % in PLLA matrix from 0 to 50 wt.%. The study showed that an increase in Hap's weight % decreased the crystallinity of scaffolds, and young's modulus reached up to the level of human bone. Several researchers have also used Hap reinforcement in the PLA matrix because of its remarkable osteo-inductive and osteoconductive properties.^[15-17] Other than Hap, Drummer et al.^[18] developed a material with PLA/tricalcium phosphate. The authors found that the PLA/TCP composite has semi-crystalline behavior, and their crystallinity increased with an increase in the nozzle temperature. Murphy et al.^[19] also developed a composite of PLA/ microcrystalline cellulose (MCC) with 1, 3, and 5 wt.% of MCC. It was found that with an increase in the reinforcement of MCC, crystallinity and storage modulus increased in comparison to PLA and showed the highest value for 3 wt.% composite of PLA/MCC. In recent research findings, Jiang et al. developed scaffolds using iron and stainless steel powder reinforcement in PLA for tissue engineering applications. It was found that composite scaffolds showed better mechanical properties, and PLA/iron scaffolds showed better biological properties than PLA scaffolds. Other than bioceramics, a combination of two polymers have also been used to develop biomaterials. In this regard, Singh et al.^[20] investigated the mechanical property for chitosan-loaded PLA. It was found that the fabricated scaffolds were mechanically and biologically suitable to meet the clinical applications.

Other than scaffold fabrication, PLA biocomposites have been used in various fixation devices. In this regard, Backes et al.^[21] reinforced β -TCP into PLA to develop bioactive composite with varying percentages of 5, 10, and 25 wt.% of TCP. The results showed that the addition of TCP enhanced biological behavior but 25 wt.% composite showed a reduction in thermal stability. Five and ten wt.% of TCP-loaded PLA were used for the fabrication of a bone fixation screw, which showed good printability and accuracy. Another work of He et al.^[21] studied the mechanical and biological properties of PLA/ phosphate glass composite. It was found that milled glass fiber reinforcement had better flexural modulus than glass particle reinforcement and even had lower strength loss during degradation. This material showed the potential for the fabrication of a bone plate fixation device. Other than this, PLA has its application in the fabrication of drug delivery systems also. In this regard, Liang et al.^[22] developed an oral delivery mouthguard of PLA/PVA blend with CBS as a drug and VA, as a food flavor substitute. The materials' mechanical, thermal, and biological properties had been proved suitable in oral drug delivery. Fu et al.^[23] developed a gastric floating tablet device with PLA. It was found that the floating time in the stomach is

long, up to 3 days due to its precise design, and the release of the drug is more in double net shape device in comparison to a single net.

The above literature indicates that PLA biocomposites have wide application in the medical field. In the present work, authors proposed to use Al_2O_3 and YSZ bioinert ceramics as the reinforcements into PLA matrix. The bioinert ceramics Al_2O_3 and YSZ has load-bearing applications such as orthopedic and dental implantable medical devices. The main purpose of reinforcement of these bioceramics into PLA matrix is to study its effect on mechanical characteristics of polymer. However, their proportion needs to be controlled to reach the desired function. Initially, a low proportion has been used in the present work due to their remarkable mechanical strength. The long-term goal of this work is to use the developed biocomposite for medical application. In this context, mechanical properties such as compression, tensile, and flexural have been characterized. Scanning Electron Microscope is also used to examine the fracture of the composite specimen. Along with thermo-mechanical behavior, other characteristics such as water contact angle and in vitro degradation test has also been conducted of the newly developed PLA/ Al_2O_3 /YSZ composites fabricated through FDM printer.

2 | MATERIALS AND METHODS

2.1 | Material

PLA (Ingeo, 3052D) thermoplastic polymer pellets were purchased from Natur Tec. Pvt. Ltd., India. Alumina (molecular weight = 101.96 g/mol) and Yttria-Stabilized Zirconia (YSZ) (molecular weight = 349.03 g/mol) were used as bioceramics purchased from Otto Chemie Pvt Ltd., India. The three polymeric biocomposites have been developed from PLA by reinforcing bio-ceramics into different weight ratios (refer Table 1). This percentage of bioceramics has been selected based on preliminary experimentation. The wt.% more than 1 resulted in clogging of the single-screw extruder and resulted in non-uniform diameter of the filament which is not fit for FDM.

TABLE 1 Polymeric biocomposite composition

| S. no. | Material | PLA (wt.%) | Al_2O_3 (wt.%) | YSZ (wt.%) |
|--------|-----------------------------------|------------|--------------------------------|------------|
| 1. | PLA | 100 | - | - |
| 2. | PLA/ Al_2O_3 | 99 | 1 | - |
| 3. | PLA/YSZ | 99 | - | 1 |
| 4. | PLA/ Al_2O_3 /YSZ | 99 | 0.5 | 0.5 |

2.2 | Preparation of filament

In order to prepare the filaments, the pellets of PLA were first dried in an oven for 4 h at 50°C to remove the moisture; this prevented bubble formation. The PLA pellets were then mixed with different weight ratios of bioceramics in ball mill (refer Table 1). The single screw extruder (Make: Noztek-Pro, UK) with L/D ratio of ~18 was used to extrude the filament out. The extruder was set at a temperature of 185–190°C and the filament with diameter 1.75 ± 0.5 mm was extruded out. The filament was then made to pass through water bath and wound up onto the spool through puller. The flow chart of the development of filament has been shown in Figure 1.

2.3 | Preparation of specimen

The test specimens were fabricated using Protocentre 999 FDM 3D printer (Make: Aha 3D, Jaipur). The printer used Kisslicer software to generate the G-code files. Figure 2 showed the compression specimen on slicing software. The bed temperature and nozzle temperature were set at 95°C and 210°C, respectively. The CAD files were designed using CATIA V5. The compression, tensile, and flexural test specimens were prepared as per ASTM D695,^[24] ASTM D638,^[25] and ASTM D790,^[26] respectively. During preparation of the specimens, various parameters affect the properties of the parts like infill percentage, support structure, printing speed, and layer height, etc. The following parameters were selected based on trial experimentation and literature which supports the dimensional accuracy and strength of parts, as shown in Table 2.

2.4 | Mechanical testing

Three specimens were manufactured and tested for all tests, and the mean value was taken to enhance the data accuracy. Universal Testing Machine (Make: Instron, Model: 5982) of 100 KN load capacity^[27] was used to perform tensile and compression test with a 1 mm/min strain rate and flexural test with a 3 mm/min strain rate. The fabricated specimens are shown in Figure 3.

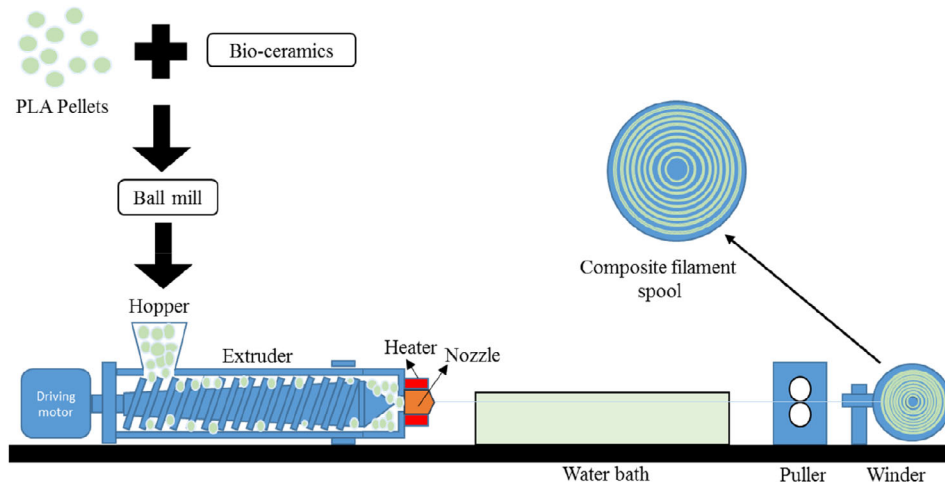


FIGURE 1 Flow chart of the development of filament [Color figure can be viewed at wileyonlinelibrary.com]

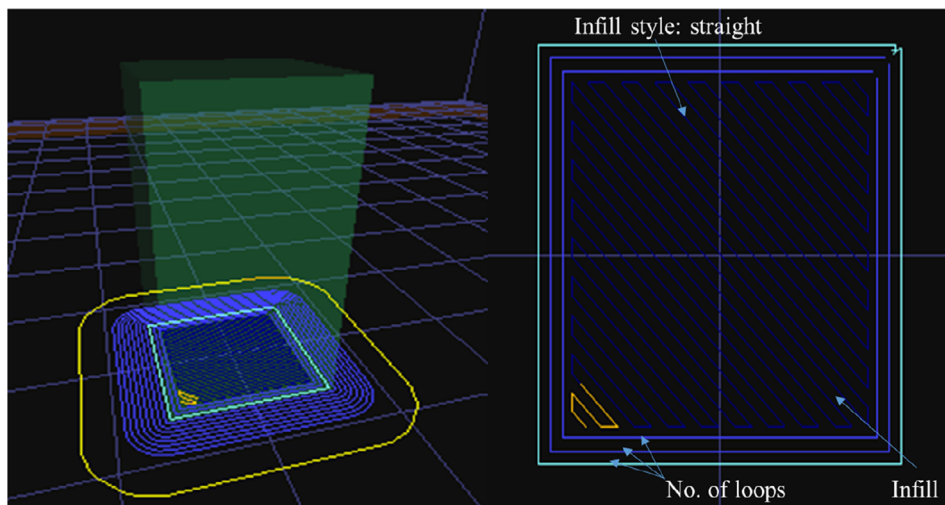


FIGURE 2 Compression test specimens on Kisslicer [Color figure can be viewed at wileyonlinelibrary.com]

TABLE 2 Process parameters used for the fabrication of test specimens

| S. no. | Parameters | Values |
|--------|-------------------|----------|
| 1. | Layer thickness | 0.1 mm |
| 2. | No. of loops | 3 |
| 3. | Infill style | Straight |
| 4. | Infill percentage | 100% |
| 5. | Print speed | 30 mm/s |

2.5 | Characterization

2.5.1 | SEM analysis of bio-ceramics

SEM has been conducted to identify the external morphology of the alumina and YSZ bio-ceramics by Carl ziess Fe-Scanning electron microscope (SEM) ultra plus with 100 KX magnification and particle size distribution was also evaluated.

2.5.2 | Thermal analysis

The thermal analysis was performed on SII 6300 EXSTAR (Make: EXSTAR). DSC and TGA techniques were used to examine characteristic temperatures and the degradation temperature of biocomposites, respectively. Samples weighing approximately 10 mg were heated with 10°C/min rate under air atmosphere. All samples were heated in the range of 25–250°C for DSC analysis and 25–700°C for TGA.

2.5.3 | Attenuated total reflection-Fourier transform infrared spectroscopy (ATR-FTIR)

ATR-FTIR was used to analyze the chemical composition of biocomposites. Tensor-II FTIR spectrometer (Make: Bruker) was used in transmittance mode with a single scan and 4 cm⁻¹ resolution. The spectrum was recorded in the range of 4500–500 cm⁻¹.

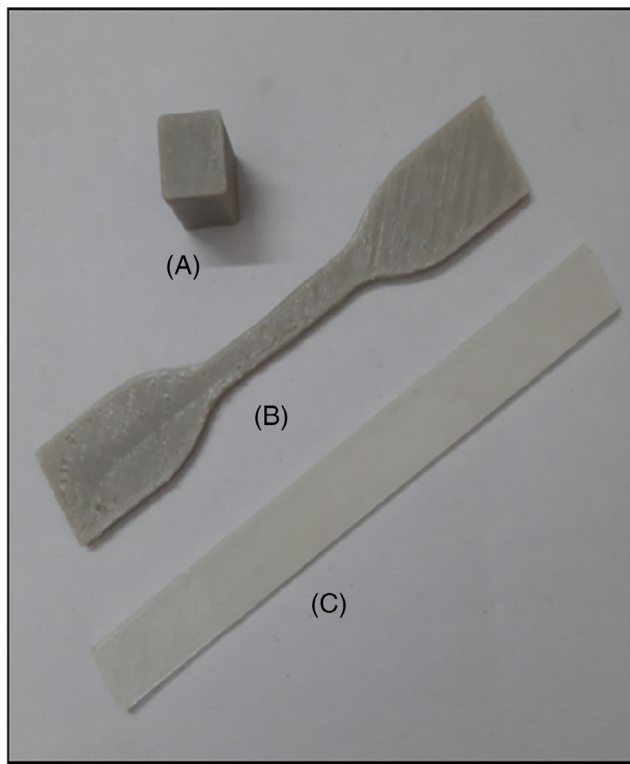


FIGURE 3 Fabricated specimens. (A) Compression test setup; (B) Tensile test setup; (C) Flexural test specimen [Color figure can be viewed at wileyonlinelibrary.com]

2.5.4 | Fractography

Fractography of tensile and flexural specimens were observed to examine the fracture surface and mode of failure using FE-SEM (Make: Carl Zeiss, Model: Ultra plus). SEM images were captured at $\times 250$ and $\times 30$ magnifications to reveal the influence of reinforcement on fabrication and fracture mechanics of specimens.

2.5.5 | Tribological test

Tribology test was performed at the pin on disc tester (Make: DUCOM TR-201LE-M8, India) with biocomposite cylindrical pin as specimens ($\phi 8\text{ mm} \times 10\text{ mm}$). The counter surface was a glass surface, which was glued to the lower plate of the machine.^[28] The friction test was performed with a normal load varying from 5 to 20 N. The rotational speed of 500 rpm and a track diameter of 60 mm for 80 s in wet condition with deionized water were selected.

2.5.6 | Water contact angle test

The wettability of the biocomposite surfaces were analyzed by measuring the contact angle with water using

EASYDROP (Make: Kruss). Deionized water droplet was deposited on the sample surface, and contact angles were measured at time interval of 5, 15, and 25 s.

2.5.7 | In vitro degradation

The degradation behavior of fabricated materials has also been assessed. The prepared samples ($10\text{ mm} \times 10\text{ mm} \times 2\text{ mm}$) were placed in 10 ml of PBS (pH = 7.4) in sealed petri dishes. These petri dishes were incubated at 37°C at 100 rpm to analyze the degradation. The weight loss (Δm) for each sample at different time intervals was calculated as per equation given below, where w_i is the initial weight and w_d is the degraded weight of the sample.

$$\Delta m = \frac{w_i - w_d}{w_i} \times 100 \quad (1)$$

3 | RESULTS AND DISCUSSION

3.1 | Morphology of bioceramics

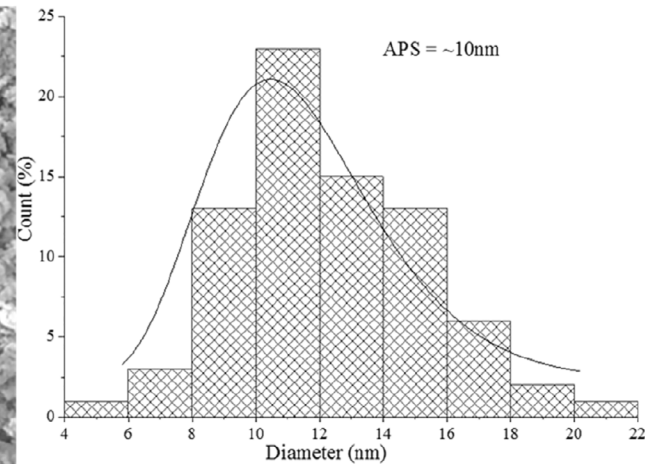
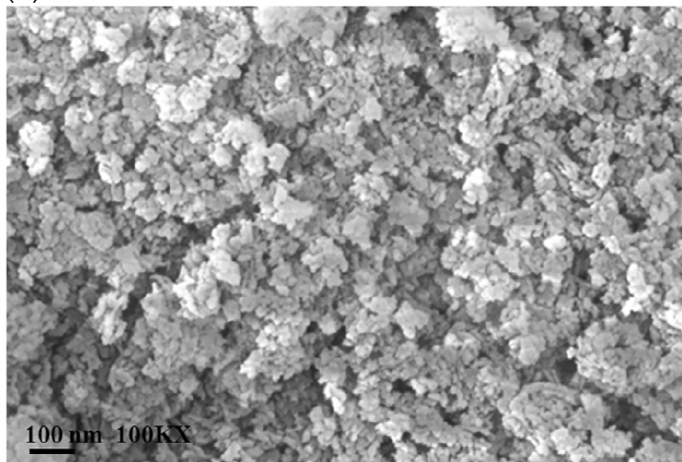
SEM images showed that bioceramics were nearly spherical in shapes and the Alumina and YSZ have average particle size of ~ 10 and ~ 50 nm, respectively (refer Figure 4).

3.2 | Thermal behavior

DSC analysis was conducted to study the influence of bioceramics on the glass transition temperature (T_g) and melting temperature (T_m) of PLA. Figure 5(A) shows that PLA has 67.25 and 151.85°C as T_g and T_m , respectively. DSC analysis revealed that the addition of different bio-ceramics did not significantly affect T_g and T_m of PLA. There has been only a 5% change in the temperature with the addition of bioceramics.

TGA profiles showed that the degradation of the material with residue is equal to zero. The TGA curves confirmed that the reinforcement of bioceramics does not affect the degradation temperature. The initial loss of material (~4%) that occurred at a temperature below 270°C is mainly because of moisture volatilization. The total decomposition of all materials occurred in the $270\text{--}370^\circ\text{C}$ temperature range, as shown in Figure 5(B).^[16] These results proved significant for the thermal evaluation of biocomposites when used in 3D printing to determine printing and decomposition temperatures.

(A)



(B)

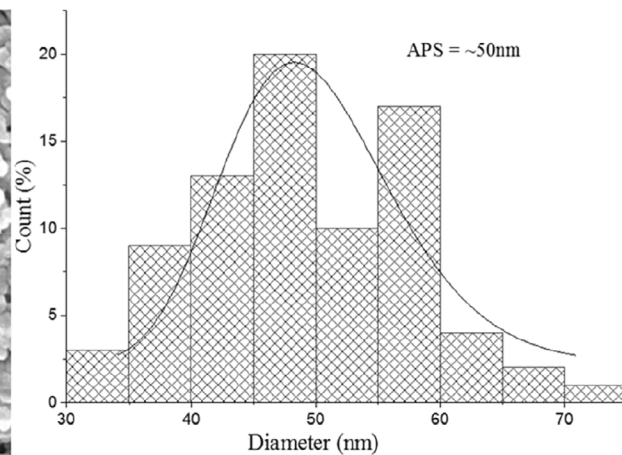
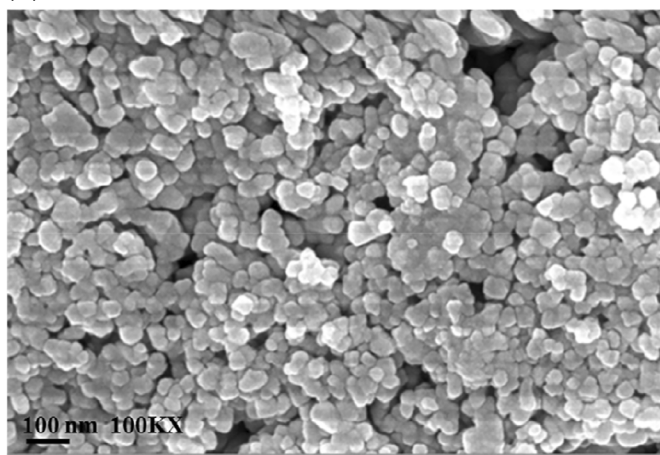


FIGURE 4 SEM images and particle size of bio-ceramics (A) alumina and (B) YSZ

3.3 | Attenuated total reflection-Fourier transform infrared spectroscopy (ATR-FTIR)

ATR-FTIR was done to examine the functional group of developed biocomposites (refer Figure 6). The band in the range of $3035\text{--}2835\text{ cm}^{-1}$ can be accounted to moisture present in the atmosphere, which showed O—H stretch. The peaks in the range $1790\text{--}1660\text{ cm}^{-1}$ and 1181 cm^{-1} belonged to C=O and C—O—C stretch of PLA. Besides this, peaks 1449 and 1081 cm^{-1} showed CH₃ asymmetrical scissoring and CH₃ symmetrical stretching, respectively.^[29] Furthermore, the spectra showed the changes in the range of $755\text{--}655\text{ cm}^{-1}$, which signifies the crystallinity change for PLA.^[30] On the addition of reinforcement, some peaks were more pronounced and clearly visible. Peaks in the range of $2319\text{--}2332\text{ cm}^{-1}$ were more prominent, showed C—O stretch.^[31] The band at 1642 cm^{-1} has been newly developed, which belonged to Zr—OH bending mode.^[32]

3.4 | Mechanical properties

The mechanical behavior of the specimens was analyzed in this work through compression, tensile, and flexural tests. The three specimens were tested for each test and mean value was taken. The data which deviated more are neglected as the liar data. The tested samples have been shown in Figure 7.

3.4.1 | Tensile test

Stress-strain curve and bar chart of average ultimate tensile strength and modulus for biocomposites have been shown in Figure 8. The results revealed that PLA has the highest average tensile strength of 31.29 MPa , and PLA/Al₂O₃ has the highest tensile modulus of 1141.4 MPa among all other compositions. Stress-strain curve for the highest deviation in strength showed that PLA/Al₂O₃ has the largest area under the curve, which

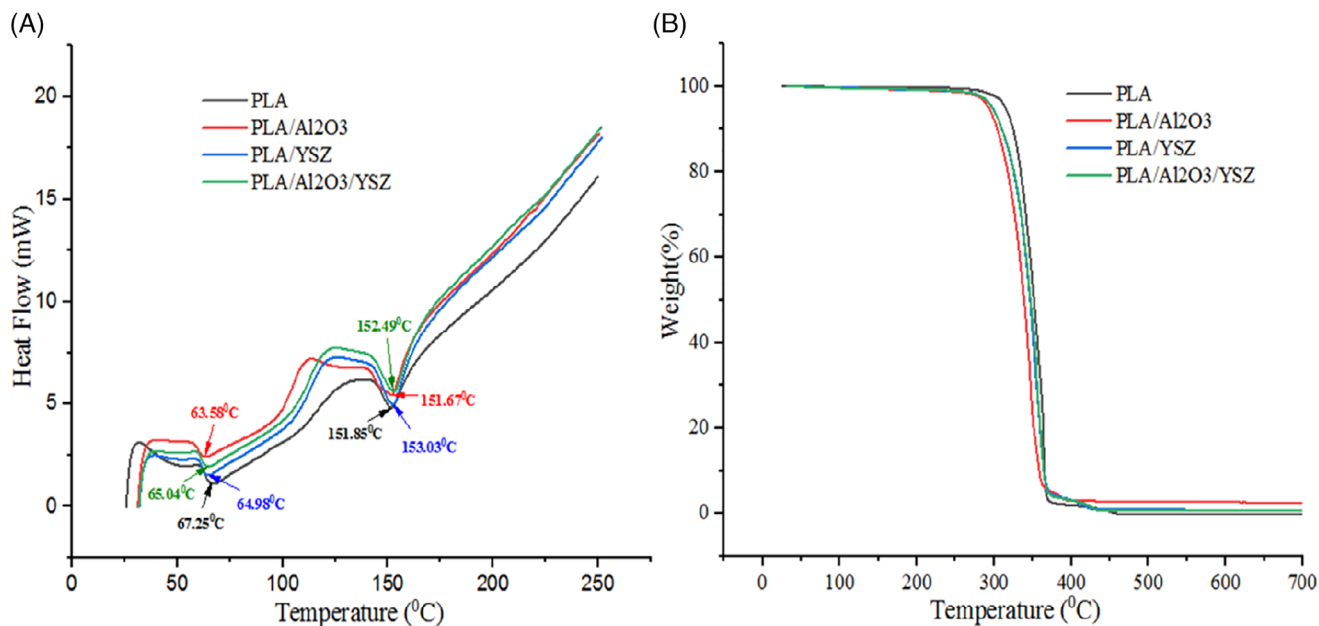


FIGURE 5 (A) Differential scanning calorimetry curves and (B) thermogravimetric analysis curves for biocomposites [Color figure can be viewed at wileyonlinelibrary.com]

shows higher toughness than PLA. PLA/YSZ has the lowest tensile strength and modulus of 15.64 and 819.2 MPa, whereas PLA/Al₂O₃/YSZ has average tensile strength and modulus of 30.05 and 1103.63 MPa, respectively.

3.4.2 | Compression test

The average ultimate compressive strength and compressive modulus with the error bar for PLA/Al₂O₃ have been the highest among all other compositions (refer Figure 9). PLA (50.61 MPa) is at the second position of compressive strength among all the tested biocomposites, followed by PLA/Al₂O₃/YSZ (48.63 MPa) and PLA/YSZ (40.99 MPa). The compressive strength, modulus, and toughness of PLA on the addition of alumina increased. This can be accounted for the fact that alumina is the most stable oxide with covalent and energetic ionic bonds, which has good compression resistance.^[33]

3.4.3 | Flexural test

Flexural strength defines the bending strength of material with combined compressive and tensile stresses. The average ultimate flexural strength of PLA (88.53 MPa) and flexural modulus of PLA/Al₂O₃ (4100.58 MPa) is higher than the rest of the compositions (refer Figure 10). Stress-strain curve has been plotted for the highest deviation in flexural strength for all biocomposites. The plot

showed that PLA/Al₂O₃ and PLA/Al₂O₃/YSZ have the highest and lowest flexural strengths, respectively. The fracture resistance strongly depends upon the flaws and defects present on the specimen tested. The variation in the strength is mainly due to the flaws present in the specimens.^[34]

In general, reinforcements should increase the mechanical properties of biocomposites from neat PLA. The present mechanical investigation concluded that the results are contradicting due to the presence of flaws in the specimens during fabrication. Instead of this, it was observed that the developed biocomposites were found to have higher strengths and modulus as compared to trabecular bone. Figure 10 shows that flexural strength is in range of that of the cortical bone for all the biocomposites. On the other hand, tensile strengths (refer Figure 8) are in close range to the trabecular bone properties.^[9,35] By suitably controlling the porosity and reinforcement %, the developed materials have the potential to be used as an alternative to the trabecular bone in the manufacturing of scaffolds for bone tissue engineering as well as orthopedic implants.

3.5 | Fractography analysis

Fractography of biocomposites was done using SEM to analyze the type and cause of fracture during mechanical tests. Figures 11 and 12 show the SEM images of fractured surfaces of biocomposites for tensile and flexural

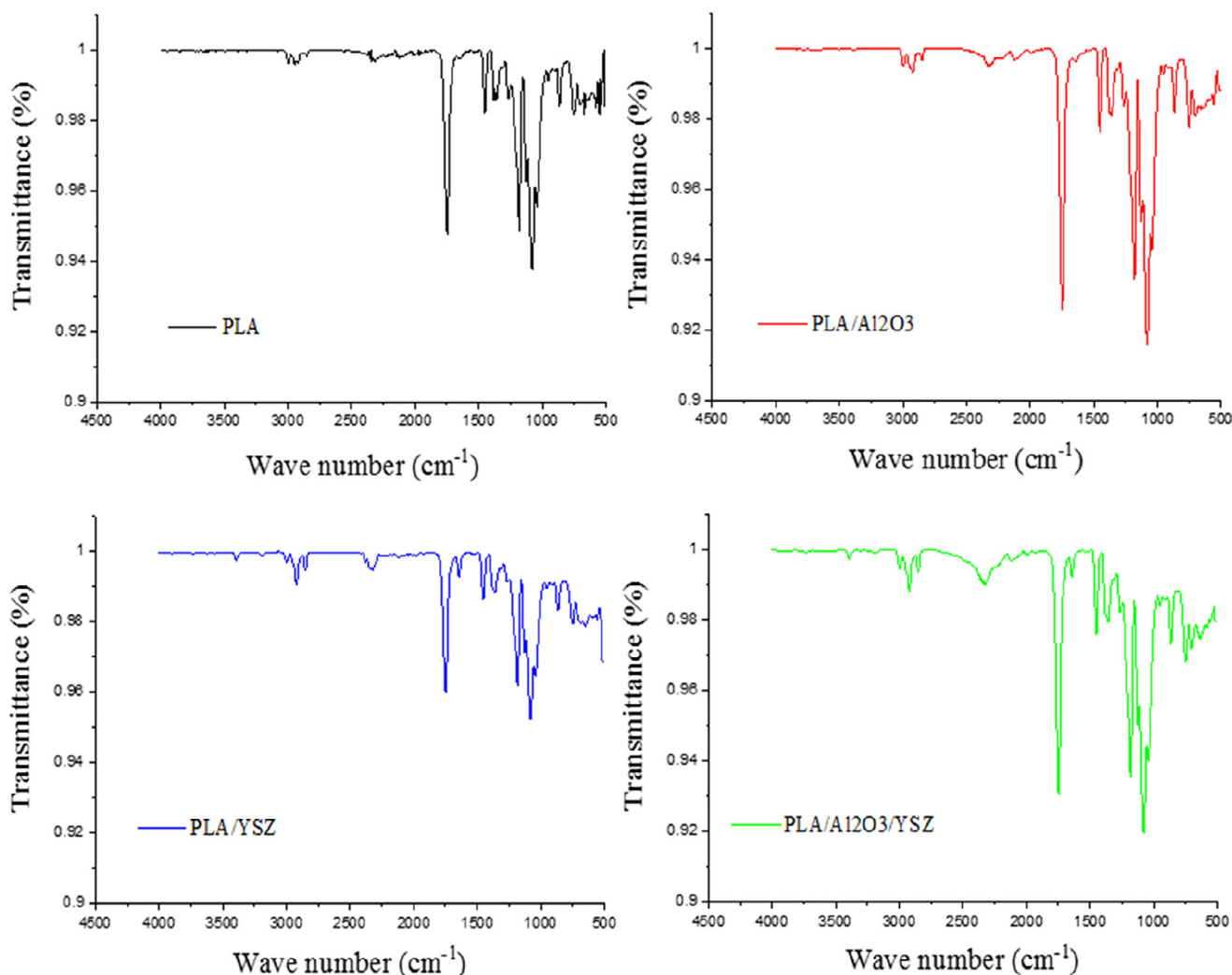


FIGURE 6 Attenuated total reflection-Fourier transform infrared spectroscopy spectra for biocomposites [Color figure can be viewed at wileyonlinelibrary.com]

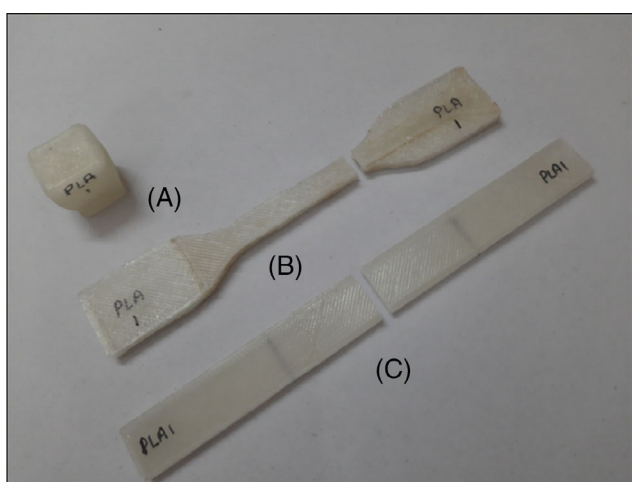


FIGURE 7 Tested samples of polylactic acid (A) compressive test specimen, (B) tensile test specimen, and (C) flexural test specimen [Color figure can be viewed at wileyonlinelibrary.com]

tests, respectively. The images clearly show that there is a brittle mode of fracture. It can be seen that reinforcements are homogeneously distributed in the polymer matrix and has proper adhesion between polymer and reinforcements. Still, there are porosities in the specimens, concluding the different composite specimens' mechanical strength variations.

In comparison to neat PLA, PLA composites have higher porosity owing to the presence of particles. Figure 11 shows that the PLA/YSZ composite has the highest porosity, and due to this, the tensile strength of this composite is the lowest (refer Figure 8). The rest of the combinations of composites has comparable porosities, and due to this, they have relatively similar tensile strength. Figure 12 reveals that PLA/Al₂O₃/YSZ has the highest porosity and comparatively least flexural strength (refer Figure 10). SEM images show that porosity is a cause to weaken the strength due to no proper cohesion

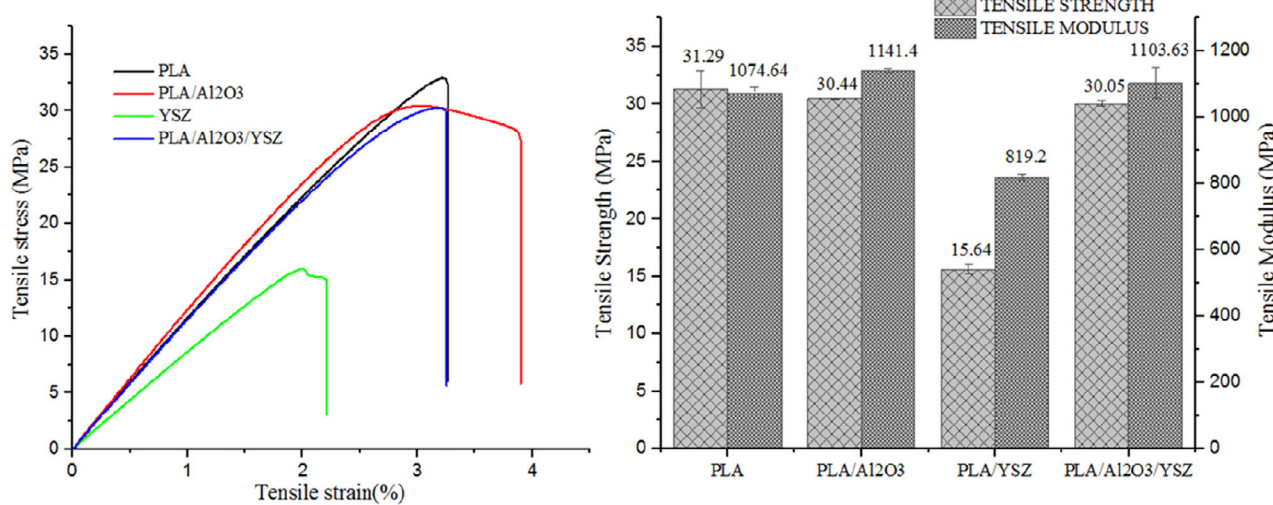


FIGURE 8 Stress–strain curve, tensile strength, and modulus for biocomposites [Color figure can be viewed at wileyonlinelibrary.com]

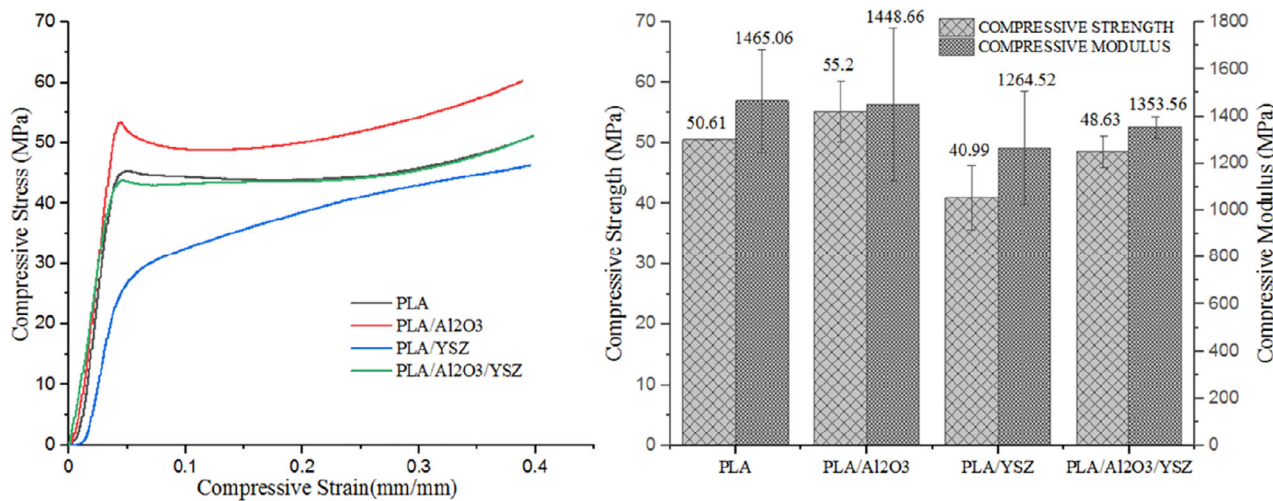


FIGURE 9 Stress–strain curve, compressive strength, and modulus for biocomposites [Color figure can be viewed at wileyonlinelibrary.com]

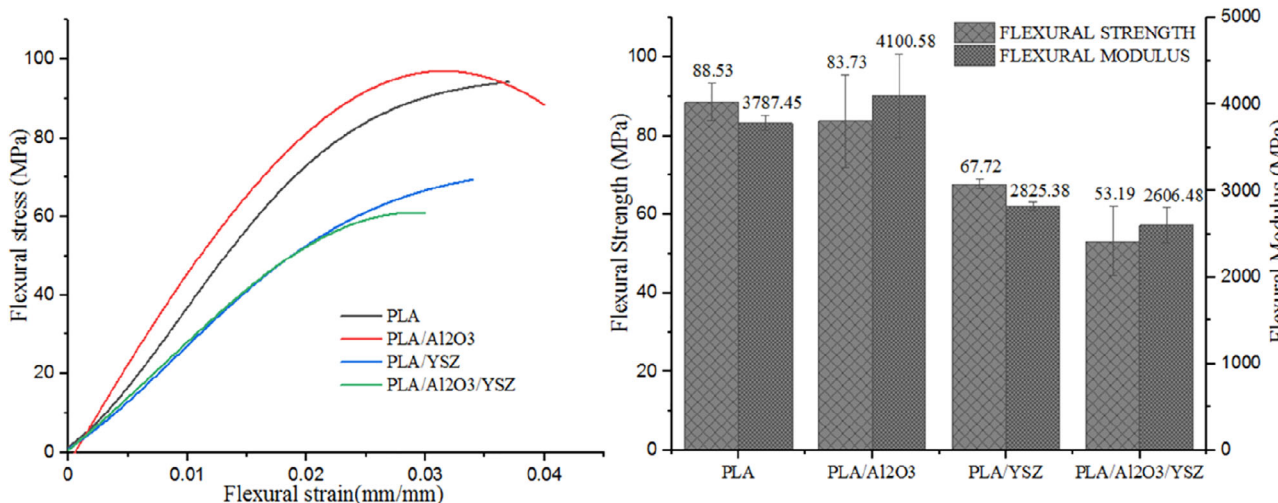


FIGURE 10 Stress–strain curve, flexural strength, and modulus for biocomposites [Color figure can be viewed at wileyonlinelibrary.com]

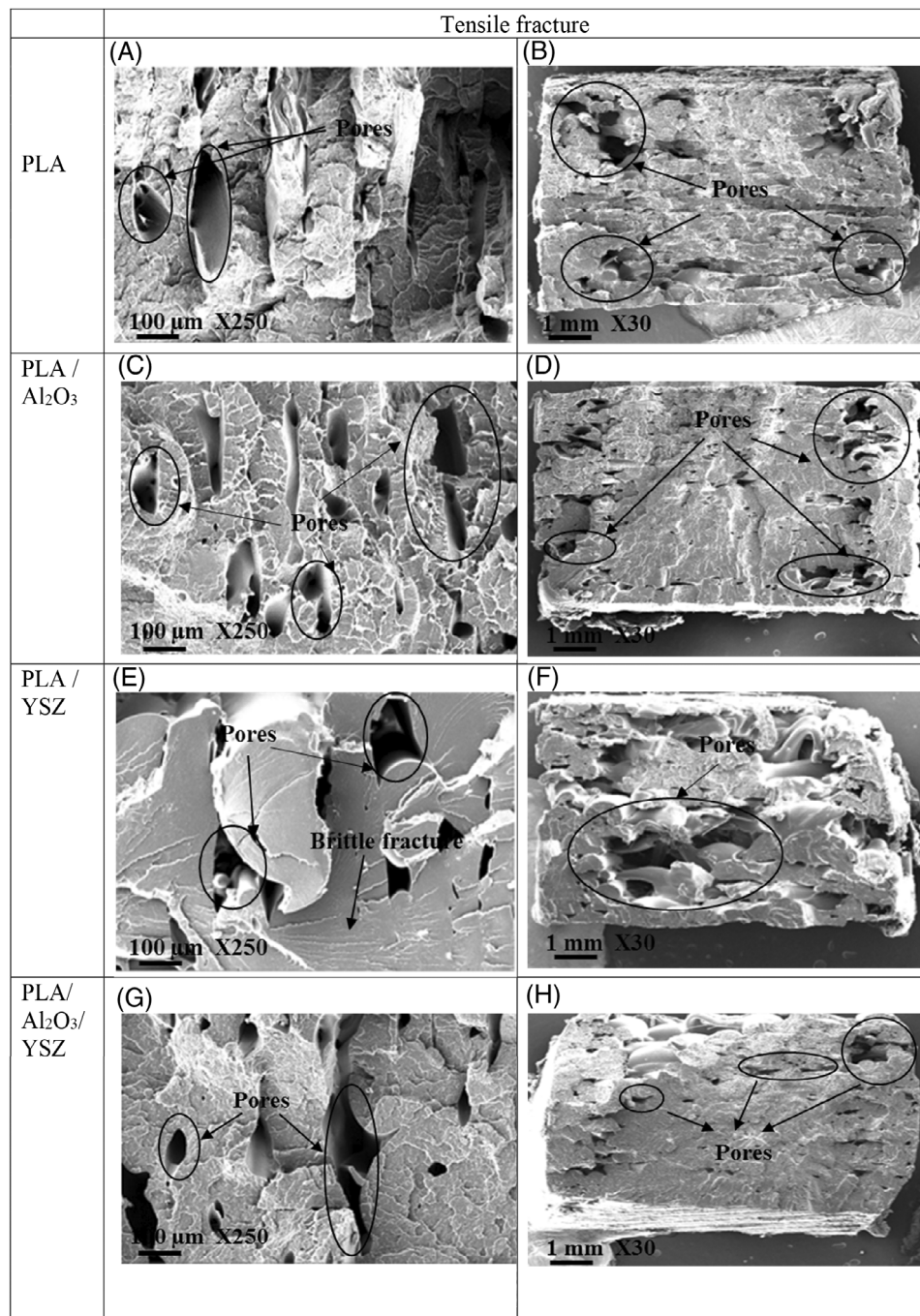


FIGURE 11 SEM images of tensile fractured specimens for biocomposites

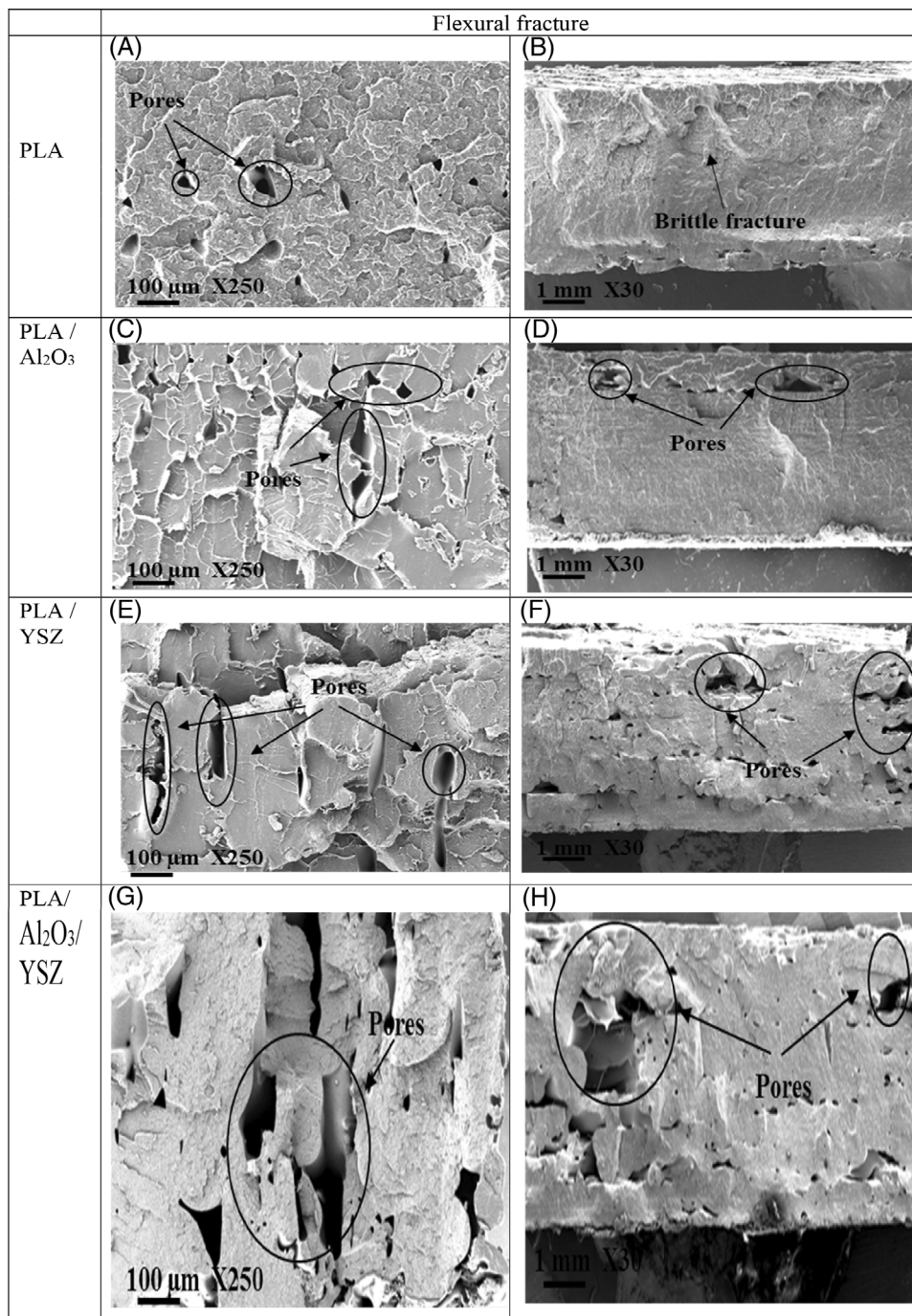
between the layers; thus, the effect of reinforcement has not been fully utilized. This can probably be addressed by optimizing the temperature during printing and particle size of reinforcement.

3.6 | Tribological behavior

Wear analysis of pin specimens against glass surface was carried out with constant speed and varying load in wet conditions. The observations after the wear analysis illustrate that initially, the coefficient of

friction (COF) between the pin and disc is high. However, with the passage of time, lubricant developed a layer between the two surfaces, due to which COF decreased. Figure 13 demonstrates that as the load increased, COF increased between the mating surfaces. At loads 15 and 20 N, COF of PLA was also considerably high due to high normal load and hence high rubbing action, but it was minimum for PLA/Al₂O₃. It showed that reinforcement of Al₂O₃ in PLA increased the wear resistance due to its remarkable hardness. Besides this, reinforcement of YSZ increased the COF, which indicated high wear. This can be accounted due

FIGURE 12 SEM images of flexural fractured specimens for biocomposites



to the low thermal conductivity of YSZ in comparison to Al₂O₃. The temperature effect is also found to increase the wear of the PLA/YSZ and thus, increased the COF.^[14]

3.7 | Contact angle test

The contact angle test was performed to investigate the wettability of biocomposites with the passage of time intervals, as shown in Figure 14. PLA and its composites

exhibit contact angle less than 90°, showing surface hydrophilicity. With an increase in time, the contact angle decreased which indicated that the water interaction with the solid surface was high. Neat PLA, PLA/Al₂O₃, PLA/YSZ, and PLA/Al₂O₃/YSZ showed contact angles of 61.6°, 71.1°, 69.9°, and 60.2°, respectively, after 25 s, as shown in Figure 15. The surface free energy can be accounted to mainly influence the wettability of solid-liquid interface mainly. High surface free energy of solid interacted more with water and spread it, resulting in lower contact angle and vice versa.^[36] The

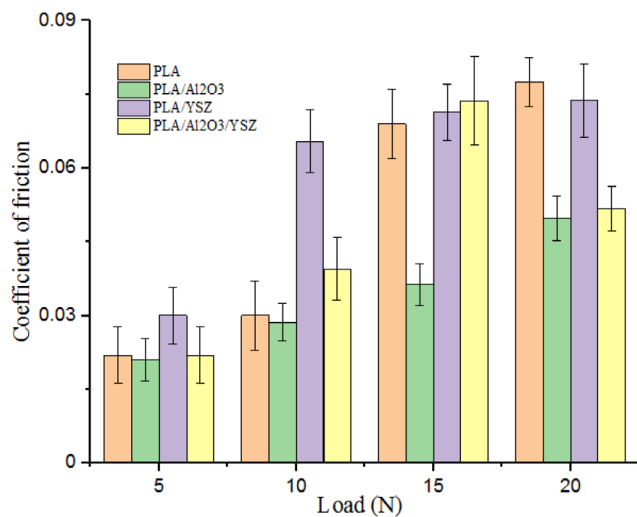


FIGURE 13 Coefficient of friction with different loads at 500 rpm [Color figure can be viewed at wileyonlinelibrary.com]

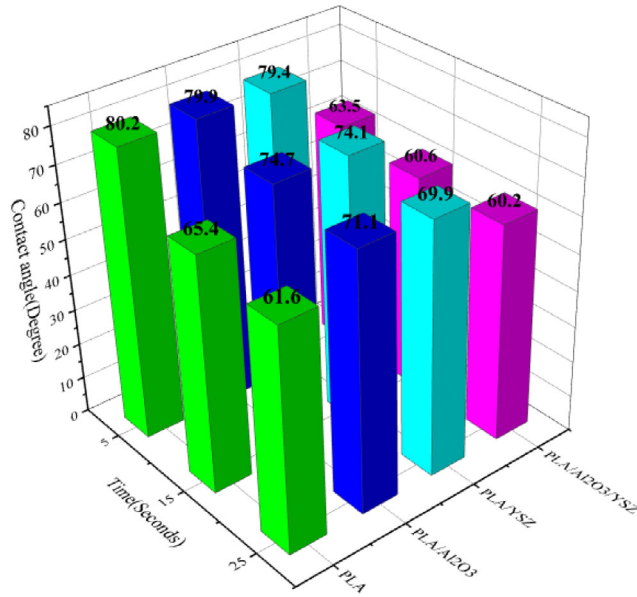


FIGURE 14 Contact angle of biocomposites with the time intervals [Color figure can be viewed at wileyonlinelibrary.com]

results show that reinforcement in PLA provides hydrophilicity, which is beneficial for biomedical applications to have cell adhesion.

3.8 | In vitro degradation behavior

The degradation of the polymeric biocomposites for 20 days has been shown in Figure 16 in terms of weight loss. It can be inferred that PLA, PLA/Al₂O₃, and PLA/YSZ offered an increasing rate of degradation with the passage of days. PLA/Al₂O₃/YSZ showed the

highest degradation initially and then constant degradation. This can be accounted due to the hydrophilic property of developed biocomposites (refer Figure 15). Al₂O₃ and YSZ have been found to have moderate degradation at room temperature. Due to this, they can have wide applications in the implant manufacturing and hard tissue engineering.^[19] Besides this, the slow degradation also provides a longer time for dense bone tissue growth.^[37]

4 | CONCLUSIONS

In the present study, mechanical and tribological behaviors of the newly developed polymeric biocomposites have been investigated. The biocomposite filaments have been developed with reinforcement of alumina and YSZ into PLA through the extrusion process. The following conclusions can be made from the present study:

1. Thermal analysis of developed biocomposite reveals that reinforcement does not change the glass transition and melting temperature substantially. TGA demonstrates that the total decomposition of the biocomposites takes place beyond 270°C. ATR-FTIR analysis showed a change in the band of spectra of PLA with reinforcement of bioceramics.
2. The mechanical investigation showed that PLA/Al₂O₃ has comparable tensile and flexural strengths with PLA and the highest compressive strength. Tensile, compressive, and flexural strengths for PLA/Al₂O₃ are 30.44, 55.2, and 83.73 MPa, respectively. PLA/Al₂O₃ has highest tensile modulus (1141.4 MPa) and flexural modulus (4100.58 MPa) and highest tensile toughness also. Factography reveals that variation in the biocomposites' mechanical property is due to the porosity developed while specimens' fabrication. Fracture analysis also showed that there is a brittle mode of fracture of specimens.
3. The tribological test demonstrates that PLA/Al₂O₃ biocomposite has the lowest COF. Besides this, the reinforcement of YSZ is found to show the highest COF due to its lower thermal conductivity and hardness compared to Al₂O₃.
4. The contact angle obtained with distilled water has values <90°, which shows the hydrophilic property of biocomposites. Hydrophilic nature is suitable for cell adhesion in biomedical applications.
5. The degradation test of the polymeric biocomposites demonstrates that PLA/Al₂O₃/YSZ has the highest weight loss initially due to its good hydrophilic nature. PLA/ YSZ and PLA/Al₂O₃ have been found to have approximately the same degradation rate.

FIGURE 15 Contact angle of biocomposites at 25 s [Color figure can be viewed at wileyonlinelibrary.com]

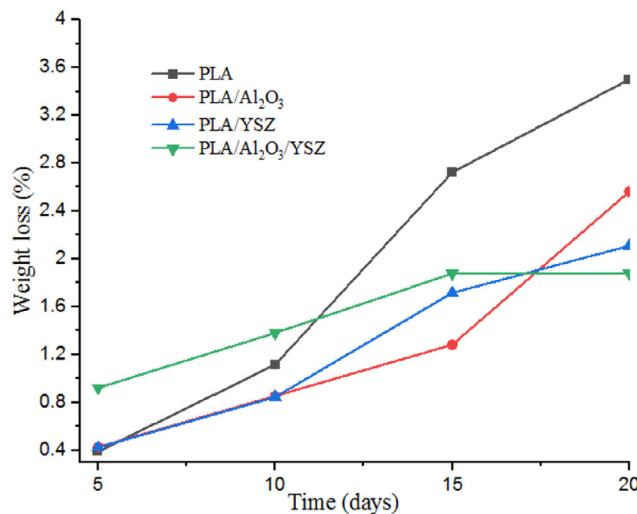
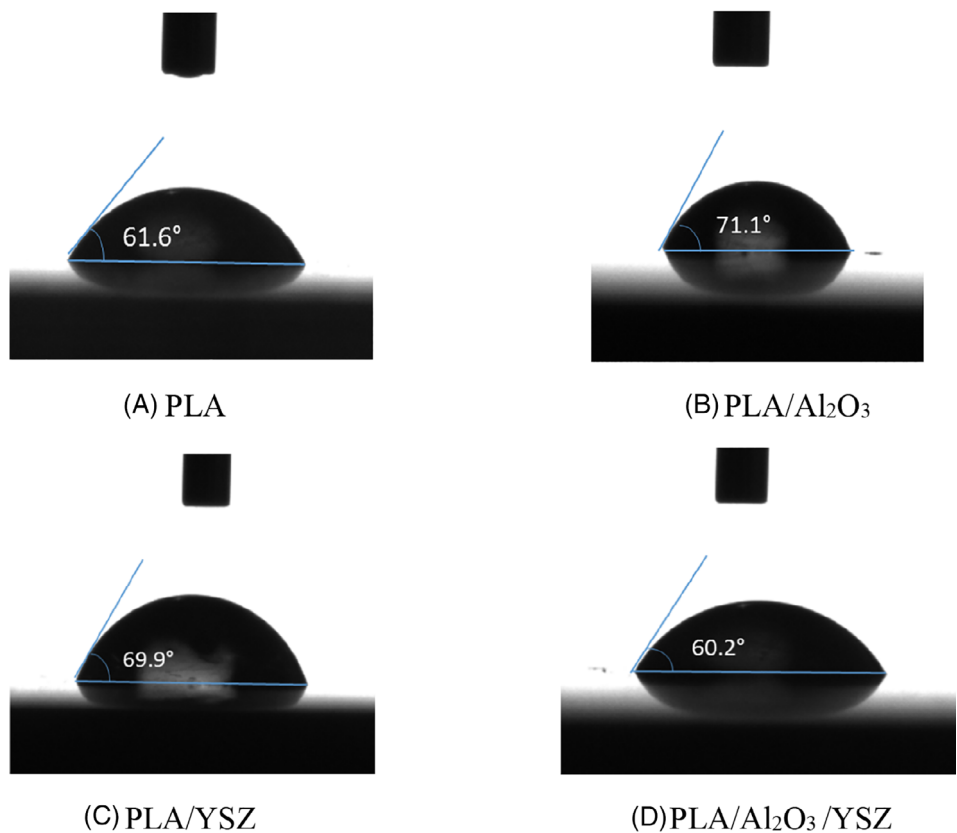


FIGURE 16 Degradation rate of biocomposites [Color figure can be viewed at wileyonlinelibrary.com]

In summary, the preliminary investigation demonstrates that PLA biocomposites have suitable mechanical and biological properties to be used in the biomedical field. Although further studies to show medical compatibility such as cell culture, cytotoxicity test, swelling index etc. and variation in weight percentage of reinforcements for mechanical strength are still required and provide the future scope in this work.

ACKNOWLEDGMENTS

The authors would like to gratefully acknowledge the financial support provided by UCOST, Dehradun, and SERB, DST, India. The funding provided by IITR is also acknowledged.

ORCID

Varun Sharma  <https://orcid.org/0000-0003-3778-901X>

REFERENCES

- [1] C. Abeykoon, P. Sri-Amphorn, A. Fernando, *Int. J. Light. Mater. Manuf.* **2020**, 3, 284.
- [2] O. A. Mohamed, S. H. Masood, J. L. Bhowmik, *Adv. Manuf.* **2015**, 3, 42.
- [3] S. Sanadhya, N. Vij, P. Chaturvedi, S. Tiwari, B. Arora, Y. K. Modi, *Int. J. of Scientific Progress and Research* **2015**, 12, 11.
- [4] A. A. Zadpoor, *J. Mech. Behav. Biomed. Mater.* **2017**, 70, 1.
- [5] S. K. Hedayati, A. H. Behravesh, S. Hasannia, A. Bagheri Saed, B. Akhoundi, *Polym. Test.* **2020**, 83, 106347.
- [6] K. R. Kunduru, A. Basu, A. Domb, *J. Encycl. Polym. Sci. Technol.* **2016**, 1.
- [7] Z. Liu, Q. Lei, S. Xing, *J. Mater. Res. Technol.* **2019**, 8, 3741.
- [8] P. Wang, B. Zou, S. Ding, C. Huang, Z. Shi, Y. Ma, P. Yao, *Compos. Part B Eng.* **2020**, 198, 108175.
- [9] P. Kumar, B. S. Dehiya, A. Sindhu, *Int. J. Appl. Eng. Res.* **2018**, 13(5), 2744.
- [10] L. C. Hwa, S. Rajoo, A. M. Noor, N. Ahmad, M. B. Uday, *Curr. Opin. Solid State Mater. Sci.* **2017**, 21, 323.

- [11] J. Wu, N. Chen, F. Bai, Q. Wang, *Polym. Compos.* **2018**, *39*, E508.
- [12] J. H. Shim, J. Y. Won, J. H. Park, J. H. Bae, G. Ahn, C. H. Kim, D. H. Lim, D. W. Cho, W. S. Yun, E. B. Bae, C. M. Jeong, J. B. Huh, *Int. J. Mol. Sci.* **2017**, *18*, 899.
- [13] S. Mondal, T. P. Nguyen, V. H. Pham, G. Hoang, P. Manivasagan, M. H. Kim, S. Y. Nam, J. Oh, *Ceram. Int.* **2020**, *46*, 3443.
- [14] N. Krishnamurthy, M. S. Prashanthareddy, H. P. Raju, H. S. Manohar, *ISRN Ceram.* **2012**, *2012*, 1.
- [15] B. I. Oladapo, I. A. Daniyan, O. M. Ikumapayi, O. B. Malachi, I. O. Malachi, *Polym. Test.* **2020**, *83*, 106341.
- [16] C. Esposito Corcione, F. Gervaso, F. Scalera, S. K. Padmanabhan, M. Madaghiele, F. Montagna, A. Sannino, A. Licciulli, A. Maffezzoli, *Ceram. Int.* **2019**, *45*, 2803.
- [17] R. H. A. Haq, M. N. A. Rahman, A. M. T. Ariffin, M. F. Hassan, M. Z. Yunos, S. Adzila, *IOP Conf. Ser.: Mater. Sci. Eng.* **2017**, *226*, 012038.
- [18] D. Drummer, S. Cifuentes-Cuéllar, D. Rietzel, *Rapid Prototyp. J.* **2012**, *18*, 500.
- [19] C. A. Murphy, M. N. Collins, *Polym. Compos.* **2018**, *39*, 1311.
- [20] S. Singh, G. Singh, C. Prakash, S. Ramakrishna, L. Lamberti, C. I. Pruncu, *Polym. Test.* **2020**, *89*, 106722.
- [21] E. H. Backes, L. Nóbile Pires, H. S. Selistre-de-Araujo, L. C. Costa, F. R. Passador, L. A. Pessan, *J. Appl. Polym. Sci.* **2021**, *138*, 49759.
- [22] K. Liang, S. Carmone, D. Brambilla, J. C. Leroux, *Sci. Adv.* **2018**, *4*, 1.
- [23] J. Fu, H. Yin, X. Yu, C. Xie, H. Jiang, Y. Jin, F. Sheng, *Int. J. Pharm.* **2018**, *549*, 370.
- [24] ASTM International ASTM D695-15 **2010**, 1.
- [25] ASTM International ASTM D638-14 **2006**, 1.
- [26] ASTM International ASTM D790 **2002**, 1.
- [27] A. Pandey, G. Singh, S. Singh, K. Jha, C. Prakash, *J. Mech. Behav. Biomed. Mater.* **2020**, *108*, 103781.
- [28] D. Warnecke, N. B. Schild, S. Klose, H. Joos, R. E. Brenner, O. Kessler, N. Skaer, R. Walker, M. Freutel, A. Ignatius, L. Dürselen, *Tribol. Int.* **2017**, *109*, 586.
- [29] A. Enumo, I. P. Gross, R. H. Saatkamp, A. T. N. Pires, A. L. Parize, *Polym. Test.* **2020**, *88*, 106552.
- [30] J. E. Martín-Alfonso, J. Urbano, A. A. Cuadri, J. M. Franco, *Polym. Test.* **2019**, *73*, 268.
- [31] Z. Elassal, L. Groula, K. Nohair, A. Sahibed-dine, R. Brahmi, M. Loghmarti, A. Mzerd, M. Bensitel, *Arab. J. Chem.* **2011**, *4*, 313.
- [32] D. Müller, S. Heuss-Aßbichler, *J. Eur. Ceram. Soc.* **2016**, *36*, 3495.
- [33] C. Piconi, G. Maccauro, F. Muratori, E. B. D. E. L. Prever, *J. Appl. Biomater. Biomech.* **2003**, *1*, 19.
- [34] C. Volpato, L. Garbelotto, M. Fredel, F. Bondioli, *Advances in Ceramics—Electric and Magnetic Ceramics, Bioceramics, Ceramics and Environment*. Intechopen, London, UK **2011**, p. 397.
- [35] L. C. Gerhardt, A. R. Boccaccini, *Materials (Basel)* **2010**, *3*, 3867.
- [36] M. L. González-Martín, L. J. Labajos-Broncano, *J. Mater. Sci.* **1999**, *34*, 5923.
- [37] S. Hassanajili, A. Karami-Pour, A. Oryan, T. Talaei-Khozani, *Mater. Sci. Eng. C* **2019**, *104*, 109960.

AUTHOR BIOGRAPHIES

Neha Choudhary is a research scholar at Department of Mechanical and Industrial Engineering at IIT Roorkee, India.

Varun Sharma is an Assistant Professor at Department of Mechanical and Industrial Engineering at IIT Roorkee, India.

Pradeep Kumar is a Professor at Department of Mechanical and Industrial Engineering at IIT Roorkee, India.

How to cite this article: N. Choudhary, V. Sharma, P. Kumar, *J Vinyl Addit Technol* **2021**, 1. <https://doi.org/10.1002/vnl.21837>